applied sciences

MDPI

*Article*

# Influence of Cargo Luggage on the Vertical Drop Crashworthiness of Aircraft Mid-Fuselage Section

**Shuhua Zhu [1,*], Kai Liu [1], Xulong Xi [2], Xiaochuan Liu [2], Yukun Zhou [1], Yaoyuan Liu [1] and Mingbo Tong [1]**

[1] College of Aerospace Engineering, Nanjing University of Aeronautics and Astronautics, Nanjing 210016, China; lk0209@nuaa.edu.cn (K.L.); spectrazyk@nuaa.edu.cn (Y.Z.); sz210100@nuaa.edu.cn (Y.L.); tongw@nuaa.edu.cn (M.T.)

[2] Key Laboratory of Structural Impact Dynamics Aerospace Science and Technology, Aircraft Strength Research Institute of China, Xi'an 710065, China; 13028512013@163.com (X.X.); liuxiaochuan@cae.ac.cn (X.L.)

* Correspondence: zhushuhua@nuaa.edu.cn

**Abstract:** The evaluation of structural crashworthiness is important for the development of civil aircraft. In this study, cargo luggage was considered in the vertical drop simulation of an aircraft mid-fuselage section. First, quasi-static compression tests on three types of luggage made of different materials were conducted. Then, a finite element model (FEM) of the cargo luggage was developed with a crushable foam material in LS-PrePost4.5 software. The finite element analysis results of the luggage made of different materials were consistent with the corresponding compression experiments. Secondly, the FEM of the mid-fuselage section was established without cargo luggage. The simulated displacement and acceleration of the fuselage section were consistent with the test results. Finally, the influences of cargo luggage on the fuselage vertical drop response were studied with the FEM considering both the fuselage structure and cargo luggage. Compared with the responses of the fuselage without cargo luggage, the cargo luggage could reduce the deformation of the cargo bay and maintain the integrity of the passenger living space in the cabin at the vertical velocity of 6 m/s, even though the initial kinetic energy was higher.

**Keywords:** civil aircraft; crashworthiness; cargo luggage; fuselage section; crash response

check for updates

**Citation:** Zhu, S.; Liu, K.; Xi, X.; Liu, X.; Zhou, Y.; Liu, Y.; Tong, M. Influence of Cargo Luggage on the Vertical Drop Crashworthiness of Aircraft Mid-Fuselage Section. *Appl. Sci.* **2023**, *13*, 12921. https://doi.org/10.3390/app132312921

Academic Editor: José António Correia

Received: 5 November 2023
Revised: 27 November 2023
Accepted: 29 November 2023
Published: 2 December 2023

**Copyright:** © 2023 by the authors. Licensee MDPI, Basel, Switzerland. This article is an open access article distributed under the terms and conditions of the Creative Commons Attribution (CC BY) license (https://creativecommons.org/licenses/by/4.0/).

## 1. Introduction

With the rapid development of the aviation industry, aircraft have become indispensable means of travel. However, despite the convenience of aircraft, the extremely low survival rate of aircraft accidents is one of the major factors hindering the development of the aviation industry. In the event of an aircraft crash, it is important to help passengers evacuate from the aircraft and minimize casualties. The structural crashworthiness of civil aircraft is very important for aviation safety [1,2].

The United States and the European Union have conducted in-depth and comprehensive research on the crashworthiness of civil aircraft, conducted systematic research on crash tests and simulation analyses of entire aircraft, and performed in-depth research on structural energy absorption design [3,4].

As early as the 1970s, the Federal Aviation Administration (FAA) and NASA Langley Research Center conducted crash tests and simulation research on Boeing 707 fuselage frame segments without cargo luggage [5], Boeing 737 fuselage frame segments with auxiliary fuel tanks, and Boeing 737 fuselage frame segments with cargo luggage [6], thereby accumulating a large number of test data and simulation analysis experience to facilitate design for aircraft structural crashworthiness.

In the 1990s, the European Union conducted crash tests and simulation research on an A320's fuselage frame section without cargo luggage and made remarkable observations on the aircraft structure [7]. Gransden and Perez Galan [8,9] conducted crash tests and simulation analysis on an A320's fuselage frame section, obtained the

acceleration response at the seat rail and the energy absorption characteristics of the structure under the condition of vertical crash, and analyzed the impact of the composite structure on the failure mode and acceleration characteristics. Kumakura [10] performed YS-11 fuselage frame crash tests and simulations, obtained the structural damage mode and acceleration response at different crash velocities, and also obtained the dynamic response and passenger injury results. A comparison of the test data showed that the crash simulation model including the passenger-and-seat restraint system achieved higher accuracy. Jackson et al. [11] conducted crash tests and simulation analysis on the center wing and front fuselage frame segments of an F-28 regional airliner and obtained a finite element model (FEM) of the real dummy–seat restraint system. In 2012, the China Aircraft Strength Research Institute, along with several research institutions and universities, conducted a vertical crash test with vertical velocity of 6.85 m/s on the classic metal fuselage frame of a civil aircraft independently developed in China [12,13], and this has provided useful data for the assessment and verification of the crashworthiness of aircraft structures. The research results showed that the metal fuselage frame structure predominantly absorbed the kinetic energy of the crash impact through plastic deformation (fuselage frame, lower area of cargo hold, skin, etc.) and fuselage structure fracture (fuselage frame, lower area of the cargo hold, connecting structure, etc.) and that the auxiliary fuel tank, cargo hold luggage, etc., had a certain impact on the falling performance of the fuselage structure.

In transport aircraft, the lower structure of the cabin floor is the primary energy absorption area, whereas the cargo compartment and luggage occupy most of the space in the lower structure of the cabin floor. Therefore, the energy absorption characteristics of cargo and luggage type affect the crashworthiness of the fuselage section. However, owing to the large dispersion of cargo luggage and the difficulty in simulating the material model and material parameters, there is a lack of systematic research.

In 2000, Karen et al. [11] conducted a crash test on the fuselage section of a B737 passenger aircraft with 3229 lb cargo compartment luggage at the FAA Technology Center in the United States. A numerical simulation was performed, and the FEM and the analysis/experiment correlation were described. In addition, suggestions for improving the model to increase its relevance were also proposed. Zheng et al. [14] studied the effect of the foam filling of the cargo floor substructure on the acceleration and failure mode of the fuselage structure, and it was reported that the foam filling of the cargo floor substructure could significantly reduce the acceleration pulse transmitted to the passenger compartment floor. Hossein et al. [15] evaluated the effect of the outer reinforcing plate on the initial stiffness, ultimate strength, and failure mechanisms of tubular K-joints under axial load under ambient and different fire conditions and proposed a highly precise, practical design equation based on the yield volume model for determining the ultimate strength. Xie et al. [16] studied the impact of cargo luggage on the crashworthiness of the fuselage section. The influences of the presence and absence of luggage in the cargo hold on the deformation mode, acceleration response, and energy absorption characteristics of the fuselage structure were obtained. However, the luggage in the cargo hold was simplified as a rigid body model, and the impact of cargo stiffness and cargo energy absorption was not considered; therefore, it is necessary to further establish a more realistic model of luggage in the cargo hold to study its impact on the crashworthiness of the fuselage section. Taghipoor et al. [17] studied the energy absorption and collapse behaviors of composite-coated corrugation-reinforced cylindrical absorbers and found that the composite coating could enhance the energy absorption by up to 44% by retarding the initial peak force. Zhu [18] analyzed the crash test data of a crash test on a B737 containing cargo luggage as the standard and verified the effectiveness of the crash simulation model considering cargo luggage from three perspectives: cargo cabin crush stroke, luggage energy absorption characteristics, and acceleration response at the seat rail.

To summarize, although cargo luggage has been researched, such research is not sufficiently systematic, and more in-depth research is necessary. In this study, compression tests on three different materials of cargo compartment luggage were performed, and a simulation model of cargo luggage was established. Based on the dynamic simulation software LS-DYNA 971, an FEM of the fuselage segment with cargo luggage was established. The impact of cargo luggage on the crashworthiness of the fuselage segment was further studied by comparing the deformation, acceleration, displacement, and energy absorption of the fuselage frame during the vertical drop of the fuselage segment models with and without cargo luggage; moreover, the overload response of the passenger compartment seat rails was also compared.

## 2. Luggage Compression Test

### *2.1. Luggage Case*

To study the compressive characteristics of the luggage, a total of 10 groups (9 single suitcases and 1 group of stacked suitcases) of quasi-static compression tests were conducted. The effects of luggage material, loading velocity, and luggage placement form on the compression deformation response were considered. The overall dimensions, material, number, and mass of the luggage used in the test are shown in Figure 1. Three suitcases of different materials were used in the test, aluminum alloy, canvas fabric, and Polycarbonate (PC) plastic, and the suitcases were randomly filled with clothes and other items.

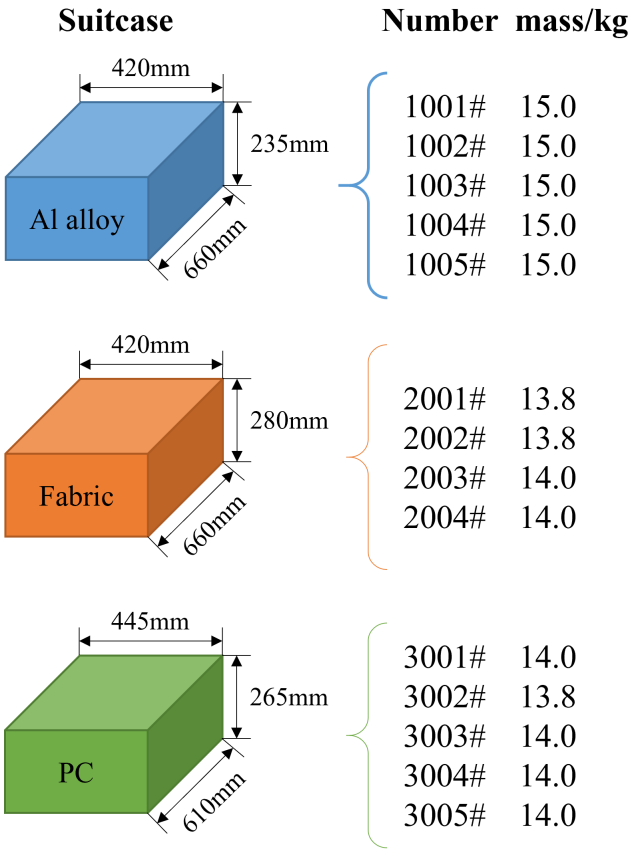



**Figure 1.** Overall dimension, material, number, and quality of the luggage.

### *2.2. Compression Test*

The testing machine in the compression test, including four columns, an upper pressing plate, a force-measuring platform, and data acquisition equipment, is shown in Figure 2a. The luggage case was compressed using the compression device, and the four columns guided the upper pressing plate to compress vertically.

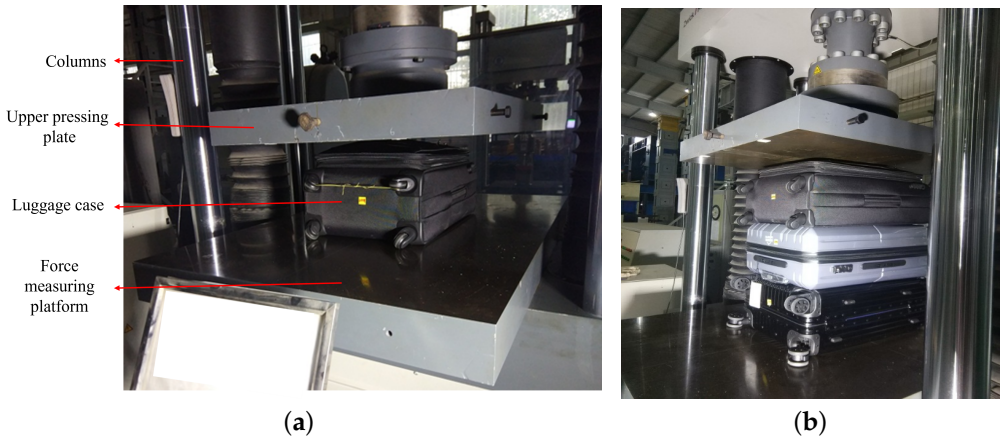



**Figure 2.** Luggage compartment arrangement. (**a**) Placed horizontally. (**b**) Stacked.

The tests were conducted at room temperature, and the suitcases were placed on the force-measuring platform, where the suitcase axis coincided with the loading axis of the testing machine. The loading velocity was also studied. The upper pressing plate of the testing machine was controlled to compress the suitcase at constant velocity (50, 150, and 300 mm/min).

During steady axial compression by the upper pressing plate, the suitcase gradually deformed until it was destroyed. The testing machine synchronously collected the curves of load and compression amount versus time, that is, the force–time curves and the displacement–time curves.

During the test, the test pieces were placed in two ways: a single test piece was placed horizontally at the center of the testing machine, and test pieces of three different materials were stacked at the center of the testing machine. The different placement methods are shown in Figure 2.

## 3. FEM of the Cargo Luggage Case

### *3.1. Modeling*

CATIA and HYPERMESH were used to establish the geometric model and the FEM of the luggage case, as shown in Figure 3a. To simulate the test process, the luggage model was placed on fixed, rigid ground, and the upper rigid plate compressed the luggage model at a certain constant velocity value, as shown in Figure 3b.

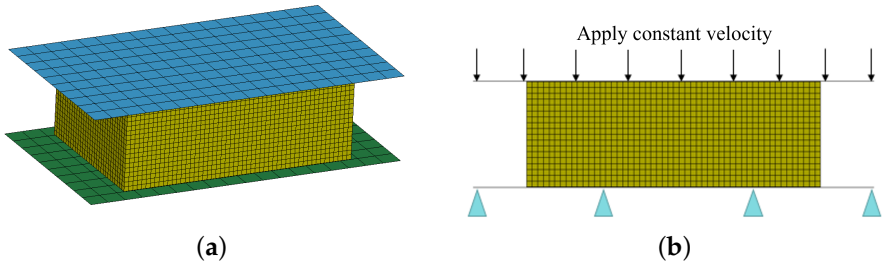



**Figure 3.** (**a**) FEM of luggage case. (**b**) Simulation of luggage compression process.

For the compression test of stacked suitcases made of three different materials, the stacked luggage was replaced by a unified overall model to consider the response of the entire cargo in the test. The FEM is shown in Figure 4. However, because the simulated luggage compartment was made of a light and soft foam material, it could easily generate negative volume in the calculation process; thus, the generation of negative volume was prevented by surrounding its shell with an outer layer. The luggage cases and rigid plates were simulated using hexahedral solid elements and quadrilateral shell elements, respectively.

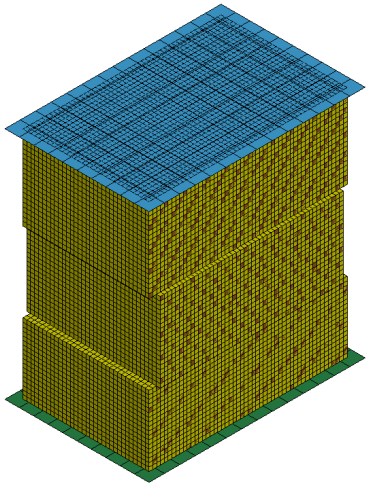


**Figure 4.** Stacked luggage compartment FEM.

### *3.2. Properties of Materials*

The compression test of luggage showed that the luggage cases were predominantly characterized by stiffness and damping, and their mechanical properties were similar to those of a foam body. Therefore, the crushable foam model MAT63_CRUSHABLE_FOAM in LS-DYNA was used to simulate the luggage. The Poisson's ratio of the crushable foam model was zero, and its stress–strain relationship is shown in Figure 5.

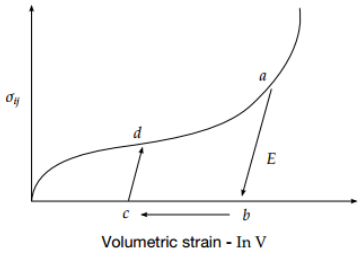



**Figure 5.** Yield stress–volume strain curve of crushable foam materials.

Figure 5 shows an example of the tensile cut-off stress (TCS) unloaded from point a to point b, then unloaded to point c, and finally reloaded to point d. At point d, the reloading continued along the loading curve. Non-zero values should be used as the TCS value to prevent material disintegration under small tensile loads. For a higher TCS value, the material exhibited a similar response behavior in both tensile and compressive states.

During the process, the model assumed that Young's modulus was constant and updated the stress by assuming elastic behavior.

$$\sigma_{ij} = \sigma_{ij}^{n} + E\varepsilon_{ij}^{(n+1)/2}\Delta t^{(n+1)/2} \tag{1}$$

Then, the principal value, $\sigma_i, i = 1, 2, 3$, was checked to see if it exceeded the yield stress, $\sigma_y$, if

$$\sigma_y < |\sigma_i| \tag{2}$$

Then, it was retracted to the yield surface:

$$\sigma_i^{n+1} = \sigma_y \frac{\sigma_i}{|\sigma_i|} \tag{3}$$

The parameters of the luggage material properties are listed in Table 1.

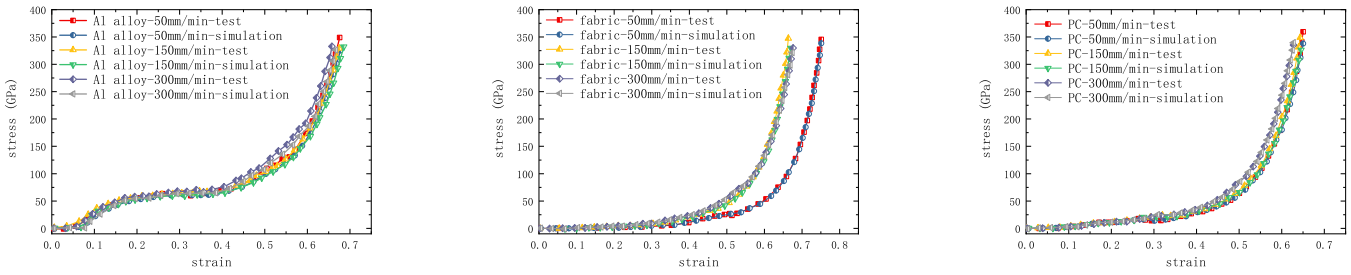
**Table 1.** Properties of luggage materials.

| Luggage Material | $\rho$/(kg/m$^3$) | *E*/GPa | PR | TSC | DAMP |
|---|---|---|---|---|---|
| Al alloy | 230.3 | 20 | | | |
| Fabric | 180.4 | 15 | 0 | $2^{-6}$ | 0.1 |
| PC | 190.6 | 18 | | | |

### *3.3. Simulation Results*

#### 3.3.1. Single-Luggage-Case Compression

The stress–strain curves obtained from the simulation calculation and test under 50, 150, and 300 mm/min working conditions for the aluminum alloy, canvas fabric, and PC plastic luggage cases are shown in Figure 6a, Figure 6b, and Figure 6c, respectively. A comparison of the stress–strain curves of the simulation and the test results under different working conditions showed that the simulation results of the three materials were highly consistent with the test results; the curves were also in good agreement.

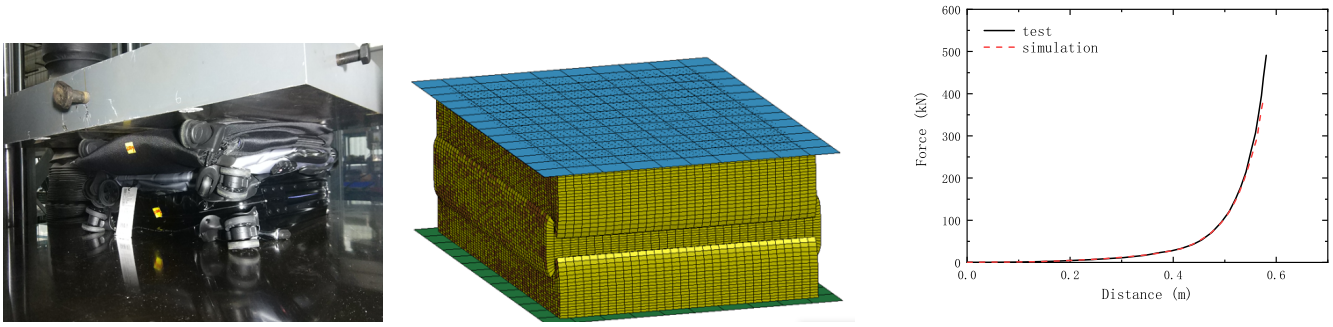



(**a**) (**b**) (**c**)

**Figure 6.** Comparison of the compression test and simulation of three different suitcases. (**a**) Aluminum alloy. (**b**) Canvas fabric. (**c**) PC plastic.

#### 3.3.2. Compression of Stacked Luggage Cases Made of Three Materials

Figure 7 shows the comparison of the stacked luggage compression test and simulation with three different materials. Figure 7a,b shows the compression deformation of the suitcases in the test and simulation, respectively. It can be seen that the deformations of the suitcases in the test and simulation were consistent. A comparison of the force–distance curves of the simulation and test (Figure 7c) of stacked luggage compression shows that the coincidence of the two curves was excellent, indicating that the simulation results of the compression process of stacked suitcases made of different materials were good.




(**a**) (**b**) (**c**)

**Figure 7.** Comparison of compression test and simulation of stacked luggagemade of three different materials. (**a**) Compression test deformation. (**b**) Compression simulation deformation. (**c**) Force–distance curve.

## 4. FEM of Mid-Fuselage without Cargo Luggage

### *4.1. Vertical Drop Test*

The vertical drop test of a civil aircraft's fuselage section was conducted at the structural crash test site of the China Aircraft Strength Research Institute [13]. The test object was a typical fuselage section structure of civil aircraft (including internal facilities).

The fuselage section model of a large civil transport aircraft was selected as the research object. The structure comprised skin, stringer, fuselage frame, floor, floor beam, etc. The distance between frames was 482.6 mm, as shown in Figure 8.

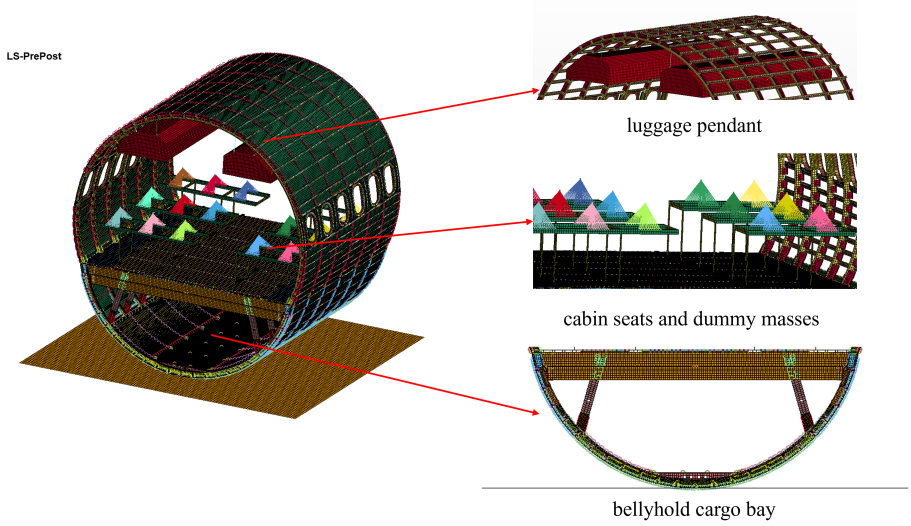



**Figure 8.** FEM of the fuselage section.

### *4.2. FEM of Fuselage Section*

The FEM of the fuselage section was established using HYPERMESH software, as shown in Figure 8. The overall FEM included the fuselage frame, stringer, skin, floor, floor beam, luggage overhead bin, seat, dummy particle, fastener, rigid ground, etc. The six degrees of freedom of the rigid floor were constrained to keep the position absolutely fixed. Gravitational acceleration of 9.8 m/s$^2$ and initial velocity of 7 m/s were applied to the entire fuselage frame segment, causing the mid-fuselage segment model to collide with the rigid floor. The SINGLE_SURFACE contact type was used inside the mid-fuselage segment, and the SURFACE_TO_SURFACE contact type was used between the fuselage segment and the floor.

The main structures of the fuselage were simulated using shell elements, and the discrete size of the structure above the cabin floor beam was 20 mm. The structure below the cabin floor beam undergoes large deformation during a crash, so the mesh size was refined to 10 mm. The dummies were simulated using concentrated masses. The mass of a single dummy was 77 kg. The mass of the dummy was bound to the rear support beam of the seat wall with a rigid node element.

The connection method for the parts of the actual airplane fuselage frame section was riveted connection. The modeling of the connections related to the main research object in the FEM was simulated using the deformable beam weld joint element (BEAM9 element), and the material model was selected as MAT100_SPOTWELD in LS-DYNA 971 software, so as to take into account the failure and energy absorption effects of the fasteners; on the other hand, for the connections between the secondary research objects, mainly the upper fuselage parts, co-node and rigid point connections were adopted.

The ground was simulated using a rigid plate. The entire model included 537,114 nodes, 479,973 shell elements, 197 concentrated mass elements, and 9297 rivet elements. The total weight of the fuselage was 1703.562 kg.

In the crash process, the mass of the luggage overhead bin and passengers' luggage imposes a large load on the fuselage frame owing to inertia; therefore, it was necessary to establish a luggage overhead bin model to evaluate the strength of the upper fuselage frame. The luggage overhead bin was separated using the shell elements, and the 5 kg luggage carried by each passenger was uniformly distributed on the surface of the luggage overhead bin using the centralized mass elements. The weight of a single overhead bin was 25.4 kg, and the total weight of the overhead bin and luggage was 125.8 kg.

### 4.3. Material Properties

Based on actual fuselage sections, Al 7075-T62 was used for the fuselage frames and stringers; Al 2024-T3571 was used for the skin and cargo floor beams; Al 7150-T77511 was used for the cabin floor beam, cabin stanchion, and cabin rail; Al 7050-T7451 was used for the windows; and sandwich wood was used for the cabin floor. The main parameters of the material properties are listed in Table 2. In the table, $\rho$ is the material density; $E$ is Young's modulus; $\sigma_y$ is the yield strength; $E_T$ is the tangent modulus; $\varepsilon_y$ is the failure strain for eroding elements.

**Table 2.** Main parameters of material properties.

| Material | $\rho$/(kg/m$^3$) | $E$/GPa | $\sigma_y$/MPa | $E_T$/MPa | $\varepsilon_y$ |
|---|---|---|---|---|---|
| 2024-T3571 | 2796 | 71 | 269 | 908 | 0.15 |
| 7075-T62 | 2796 | 71 | 441 | 937 | 0.07 |
| 7150-T77511 | 2823 | 71 | 538 | 679 | 0.07 |
| 7050-T7451 | 2768 | 71 | 441 | 679 | 0.07 |
| Sandwich wood | 497 | 40 | 178 | 150 | 0.02 |

The material model was chosen as the bilinear isotropic material model MAT3_PLASTIC_KINEMATIC in LS-DYNA 971 software. This material model is suitable for both isotropic and kinematically reinforced plasticity models and takes into account the influence of velocity effects.

### 4.4. Simulation Results

The FEM of the fuselage section was made to vertically impact the rigid ground at the initial velocity of 7 m/s, and the structural deformation, acceleration, and other simulation results of the fuselage segment were obtained. When the workstation used for simulation was configured with AMD's Ryzen 9 7950X 16-Core CPU and NVIDIA's GeForce GTX 1650 GPU, the time required to compute the model was approximately 10 h.

#### 4.4.1. Deformation

The velocity–time curves of the simulation and test are compared in Figure 9. The starting time of impact was 0 (time = 0 ms). The velocity increased as the time of impact increased. The deformation in the lower region of the fuselage frame gradually increased. The simulation and experimental curves are staggered upwards, and the trend remains identical. When the simulation and test velocity values were 0 m/s, the times were 115 ms and 122 ms respectively, with a difference of only 7 ms. The velocity of the two curves started from values greater than 0 m/s, indicating that the fuselage frame started to rebound. During rebound, the simulation velocity was slightly greater than the test velocity. This is mainly because in the simulation model, the ground model for fuselage frame impact was a rigid plate, but in the actual experiment, it was a force-measuring platform, which absorbed some energy under the large impact, which led to the rebound velocity of the simulation result in the second half of the curve being higher than the experimental result. In addition, there were model simplification, experimental environment, the initial state

of the test piece, and other aspects of the impact. In general, the simulated velocity–time curve correlated well with the test result.

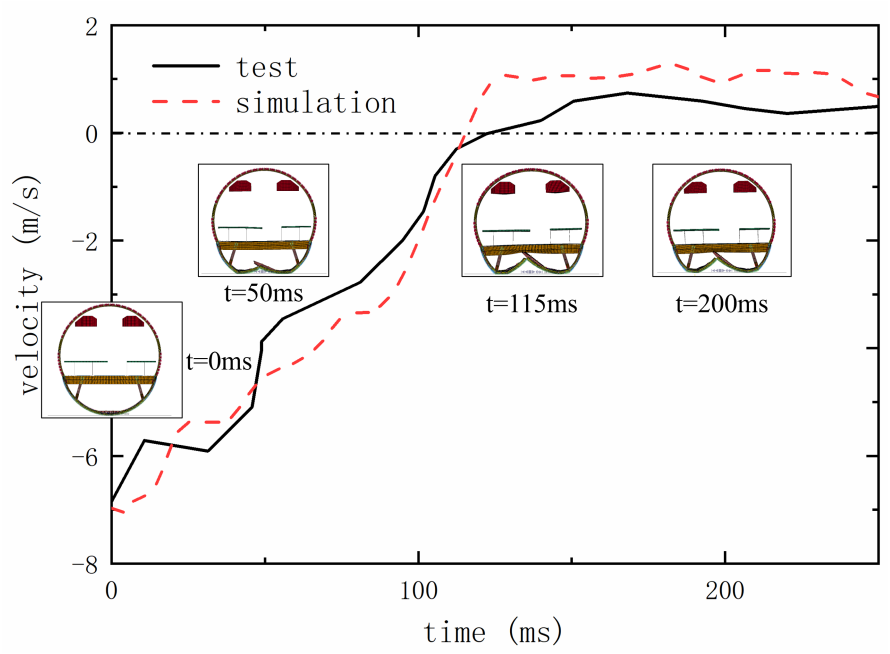
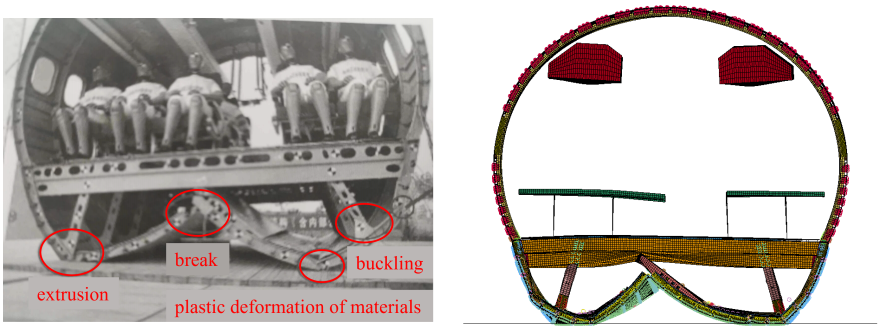



**Figure 9.** Comparison of the velocity time curves of simulation and test.

Figure 10 shows the deformation of the fuselage section in the test and simulation when the velocity was 0 m/s. Under the impact load, the cabin remained intact, and the living space of passengers remained unchanged. However, the substructure of the cabin floor was greatly deformed, and some materials of the fuselage frame were plastically deformed. The cargo floor beams broke, and the cargo floor connector was pulled off. The dummies did not collide with the structure; the restraint of the safety belts of dummies was maintained; the seat did not undergo plastic deformation; and the connection with the guide rail was maintained.




(**a**) (**b**)

**Figure 10.** Deformation of the fuselage section in the test and simulation. (**a**) Test. (**b**) Simulation.

4.4.2. Acceleration Responses

The acceleration measuring point of the passenger compartment floor plane was located at the intersection of the floor beam and seat rail. The layout of the dummies in the passenger compartment is shown in Figure 11. a–e correspond to the numbers of the floor beams. Triple seats were installed on rails 1 and 2, and double seats were installed on rails 3 and 4.

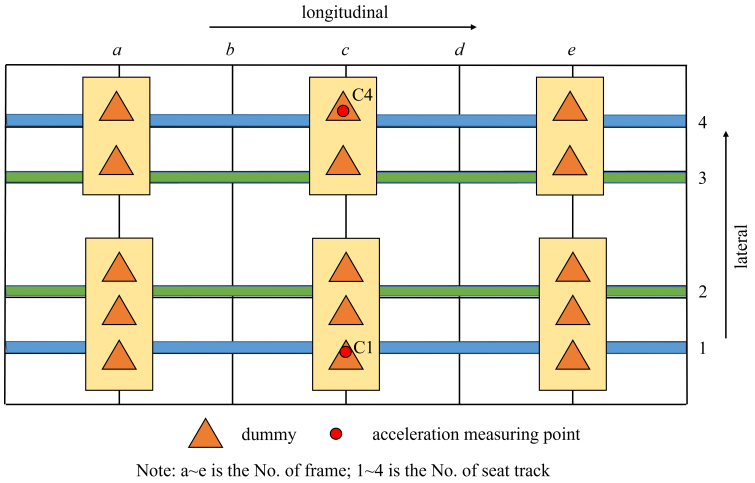



**Figure 11.** Layout of test dummies in cabin.

A comparison of the acceleration–time curves of the simulation and test at C1 (intersection of floor beam c and seat rail 1) and C4 (intersection of floor beam c and seat rail 4) is shown in Figure 12. At C1, the test initial peak acceleration was 16.2 g, and the simulation initial peak acceleration was 17.6 g, which was 8.6% higher than the test initial peak acceleration. At C4, the test initial peak acceleration was 17.1 g, and the simulation initial peak acceleration was 17.2 g, which was 0.5% higher than the test initial peak acceleration.

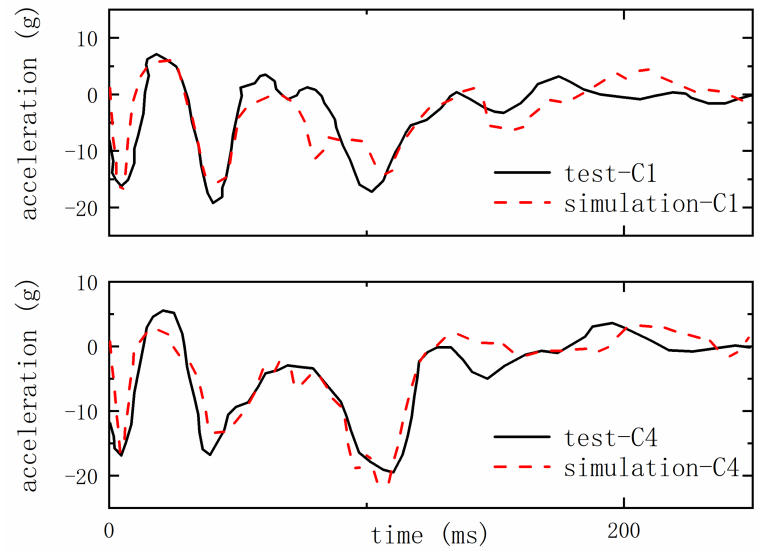



**Figure 12.** Comparison of the acceleration–time curves of the simulation and test.

## 5. Influence of Cargo Luggage on Fuselage Section Crash Response

In the process of an actual aircraft crash, the structure of the cargo hold is greatly deformed. Moreover, the cargo luggage is also crushed and damaged, absorbing crash energy. Therefore, when studying the impact factors of a crash, it is necessary to consider the impact of cargo weight and its extrusion deformation in aircraft crashes.

The total weight of the fuselage, including cargo luggage, was 2435.562 kg; the cargo luggage weighed 732 kg, accounting for 30.05% of the total weight of the fuselage. It can be seen that cargo luggage accounts for a large proportion of the total weight, and its impact on the kinetic energy of the crash cannot be ignored. Therefore, its impact on crashworthiness should be considered in crash analysis.

In this study, special compression tests were conducted on luggage, and the stress–strain curves of the luggage were obtained. A verified FEM of the fuselage section is

selected in Section 4. The FEM of the fuselage section model with cargo luggage is shown in Figure 13.

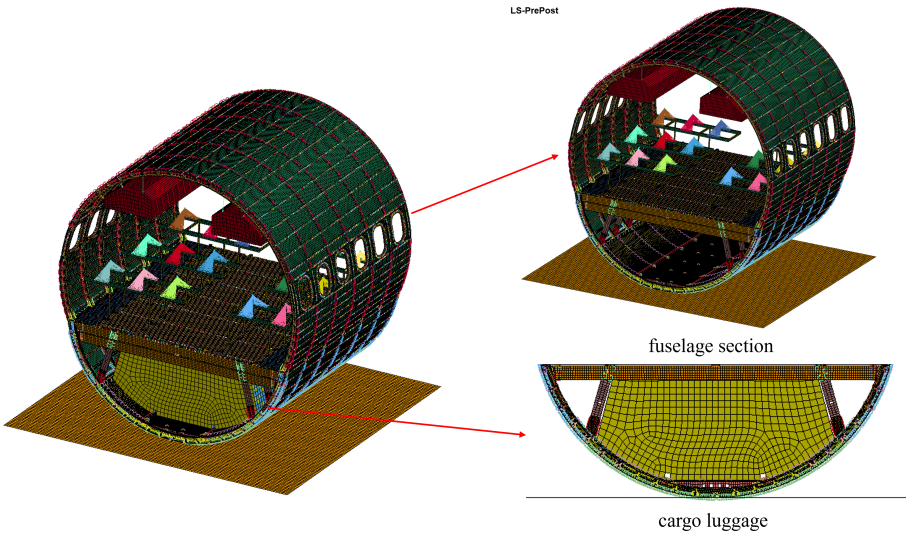


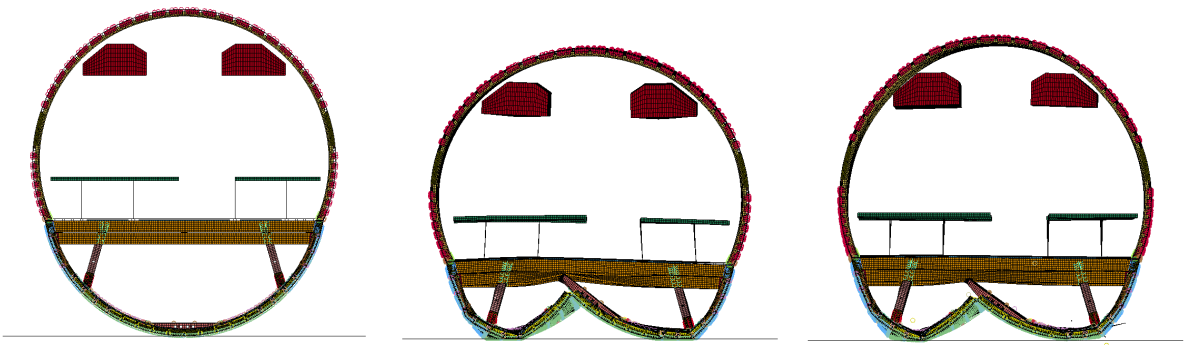

**Figure 13.** FEM of fuselage section with cargo luggage.

LS-DYNA was used to simulate the vertical crash of the fuselage section model without cargo and with cargo luggage, respectively. The vertical speed was 6 m/s. By comparing the deformation, acceleration, displacement, and energy absorption of the two fuselage segments, as well as the overload response of the passenger compartment seat rails during the vertical crash, the influence of the cargo luggage on the fuselage frame crash response was analyzed.

### *5.1. Deformation and Failure of Fuselage Frame during Vertical Crash*

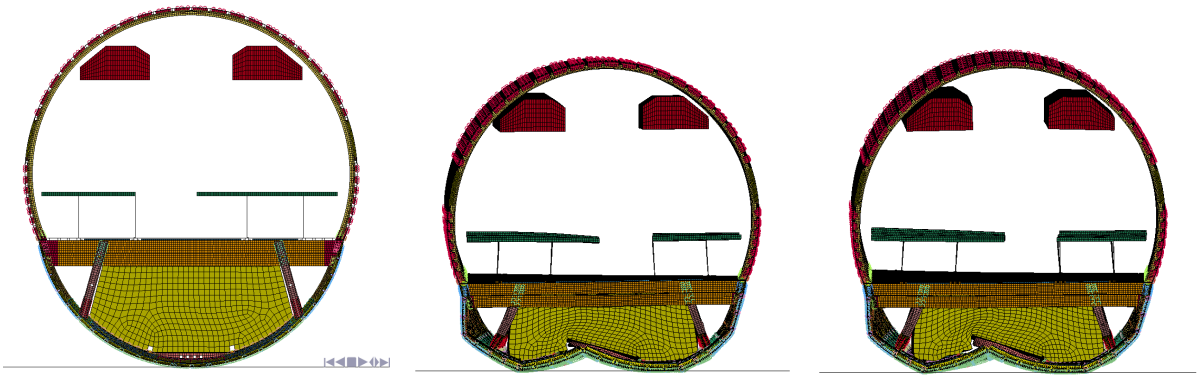
Figures 14 and 15 show the deformation diagrams of the fuselage section model without and with cargo luggage, respectively, at different times at the velocity of 6 m/s. The comparison shows that owing to the presence of luggage in the cargo hold, it was squeezed by its gravity and the cross beam of the cabin floor during the crash; moreover, the cargo luggage also had a strong squeezing effect on the cargo floor beam. Therefore, the cargo luggage limited the damage and deformation of the cargo floor beam.

When t = 0 ms, the bottom of the center fuselage segment began to come into contact with the ground. The two models remained intact without deformation. When t = 100 ms, the cargo floor without luggage was lifted to come in contact with the cabin floor and then continued being lifted, thereby easily penetrating the cabin floor and threatening passenger safety. However, owing to the presence of cargo luggage, the floor of the cargo hold was only slightly raised, and the deformation was much less than that without luggage. At 180 ms, the cargo floor deformed almost to the same extent as at 100 ms. This shows that the luggage hindered further deformation of the cargo floor as the impact time increased and that the deformation of the cargo floor did not threaten the safety of passengers in the cabin. Comparing the results with Figure 14 highlights the importance of luggage in the design of airframe crash resistance.



(**a**) (**b**) (**c**)

**Figure 14.** Deformation diagrams of fuselage frame without cargo luggage. (**a**) t = 0 ms. (**b**) t = 100 ms. (**c**) t = 180 ms.



(**a**) (**b**) (**c**)

**Figure 15.** Deformation diagrams of fuselage frame with cargo luggage. (**a**) t = 0 ms. (**b**) t = 100 ms. (**c**) t = 180 ms.

### *5.2. Acceleration Response*

The vertical acceleration curves of the fuselage section without and with cargo luggage are shown in Figure 16. At approximately 13 ms, the first peak acceleration occurred after the two models touched the ground. The acceleration of the model without cargo luggage was slightly greater than that of the model with cargo luggage. However, at approximately 60 ms, the acceleration response curve with the cargo luggage model had a secondary peak value, which was greater than the acceleration value of the model without cargo luggage at that time. This is because cargo luggage, as a relatively soft structure, plays an energy-absorbing and buffering role in the crash process but it limits the subsequent deformation of the lower structure of the cargo hold floor, rendering it impossible for the lower structure to absorb the impact through further deformation. At approximately 103 ms, a small peak was observed in the acceleration response curve in the model without cargo luggage, and this was caused by the cargo floor tilting and coming into contact with the cabin floor. At approximately 148 ms, the pillars on both sides of the cargo hold of the model without cargo luggage touched the ground, resulting in the final peak of the curve; then, the acceleration gradually stabilized at about 0. As the cargo luggage had the function of energy absorption and buffering, the deformation of the fuselage frame was small; thus, the last two peaks relative to the curve without cargo luggage were not present here. After 75 ms, the acceleration gradually decreased and finally stabilized at approximately 0 g.

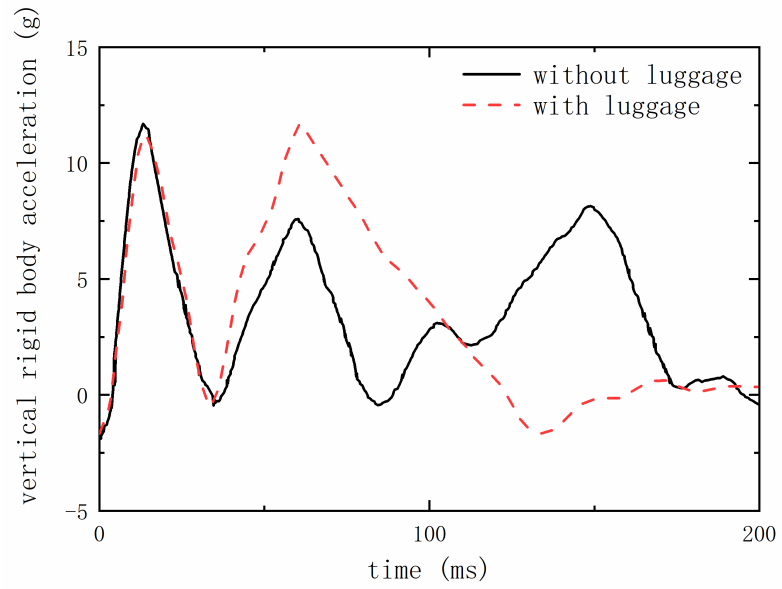



**Figure 16.** Comparison of the vertical acceleration curve of the fuselage section without and with cargo luggage.

From the perspective of the total vertical rigid body acceleration, although the presence of cargo luggage increased the initial crash kinetic energy and also inhibited the deformation and energy absorption of the substructure of the cargo floor, cargo luggage had a certain energy-absorbing and buffering effect.

### *5.3. Vertical Displacement Response*

The vertical displacement curves of the fuselage section without and with cargo luggage are shown in Figure 17. The maximum displacement value of the fuselage with cargo luggage was 234 mm when t = 90 ms, and that of the fuselage without cargo luggage was 433 mm when t = 150 ms. This shows that the vertical displacement of the fuselage section with cargo luggage is less than the vertical displacement without cargo luggage; thus, the presence of luggage ensures the integrity of the passenger living space of the cabin structure to the greatest extent.

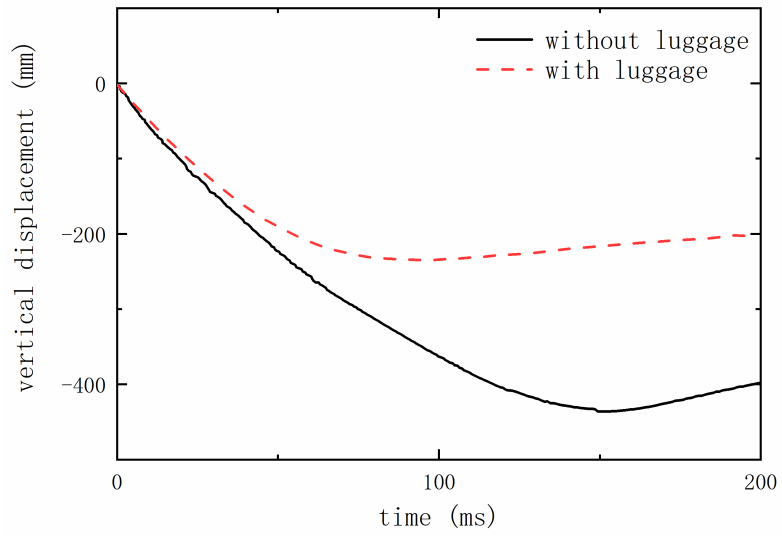



**Figure 17.** Vertical displacement curves of fuselage section without and with cargo luggage.

### *5.4. Energy Absorption Characteristics*

The structures under the cabin floor are the primary parts that absorb energy during a crash. When an aircraft crash-lands during an emergency, the stronger the energy absorption capacity of the structures under the cabin floor, the lower the impact of the kinetic energy transferred to the cabin area, and the higher the probability of safe survival of the passengers. Therefore, the evaluation of the energy absorption capacity of the main energy-absorbing components of the fuselage should be focused on the evaluation of the crashworthiness of an aircraft.

During the vertical crash of the fuselage section, the fuselage frame, skin, cargo luggage, joints, and cargo floor beam are the main deformation structures. The energy absorption ability of these components affects the crashworthiness of the fuselage. Figure 18 shows the proportion and value of the energy absorption of each component. The energy absorption of the cargo luggage was the greatest, and the maximum energy absorption was 14,900 J, which accounted for 39.2% of the total energy absorption. The energy absorption of the fuselage frame was the second largest, and the energy absorption was 5270 J, accounting for 13.9% of the total energy absorption. Moreover, 74.84% of the total energy was absorbed by the cargo luggage, fuselage frames, fasteners, and skin, which were the main energy absorption components. The energy absorption of fasteners accounted for 11.4% of the total energy absorption. This shows that the modeling of structural fasteners cannot be ignored when the accuracy of the simulation analysis of structural energy absorption design is required to be high in a crashworthiness study.

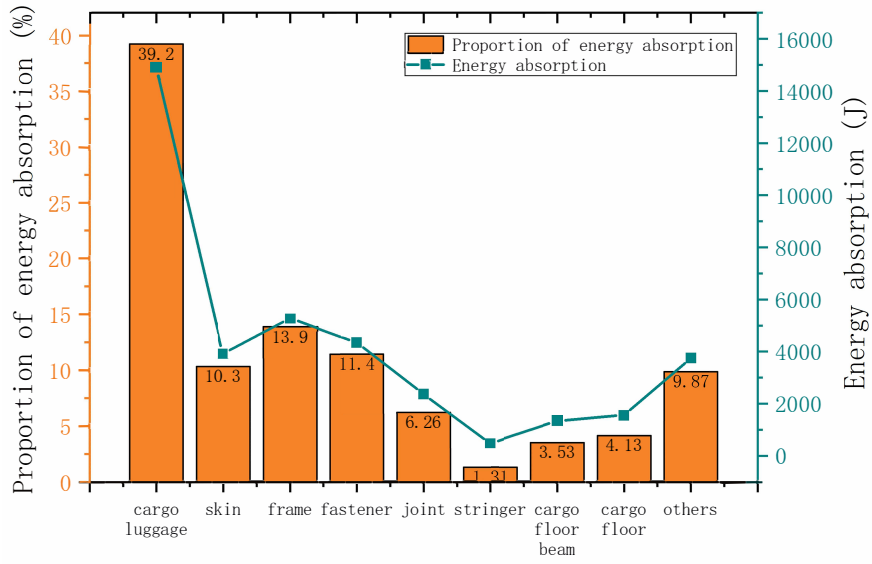



**Figure 18.** Proportion and value of energy absorption of each component.

### *5.5. Acceleration Response of Passenger Seat Rail*

To study the load transmitted from the fuselage cargo structure to the cabin during the crash, the acceleration response of the cabin seat rail was mainly studied. A total of six acceleration measuring points were selected on the inner floor guide rail of the cabin, as shown in Figure 19. The vertical lines in Figure 19 represent the fuselage frames, and the numbers are FS1-FS7 from left to right. The green and blue lines in the horizontal direction indicate the inner and outer floor guide rails of the cabin, respectively. The six acceleration measuring points are located at the intersection between fuselage frames FS2, FS4, and FS6 and the inner floor guide rail of the cabin, respectively.

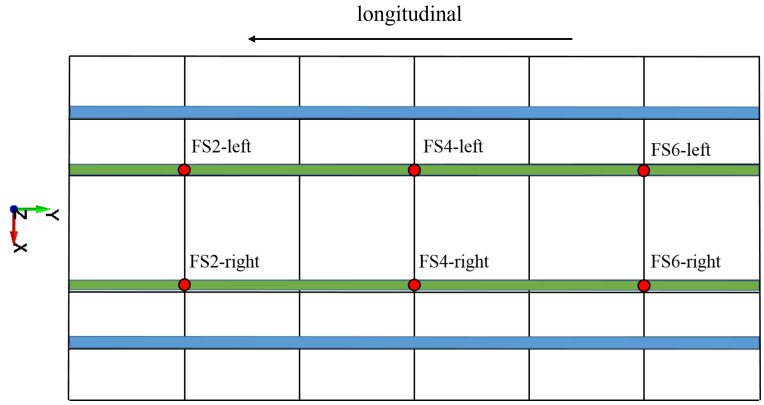



**Figure 19.** Schematic of selection of the acceleration measuring points of passenger seat rail.

The acceleration response curves of the models of the passenger cabin seat rail without and with cargo are compared in Figure 20. The comparison shows that although the acceleration of the fuselage without cargo luggage was slightly greater than that of the fuselage with cargo luggage when the first overload peak occurred, the second overload peak of the model with cargo luggage was greater than that of the model without cargo luggage and subsequently reached the maximum value of acceleration there. Therefore, cargo luggage increases the overload suffered by passengers in a vertical crash.

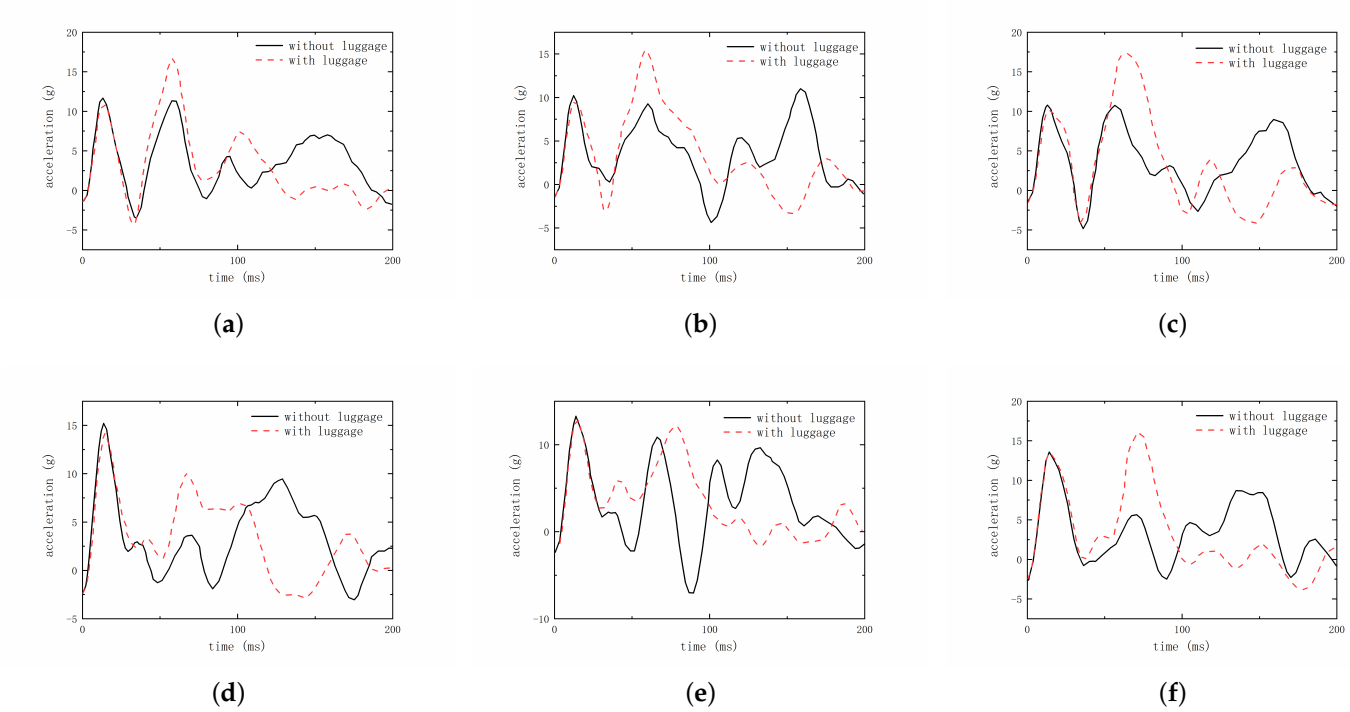



**Figure 20.** Comparison of acceleration responses of guide rail with and without cargo luggage in the fuselage section. (**a**) FS2-left. (**b**) FS4-left. (**c**) FS6-left. (**d**) FS2-right. (**e**) FS4-right. (**f**) FS6-right.

According to the technical index of the overload tolerance limit of the human body in all directions in CCAR-25, the airworthiness standard of transport aircraft in China, the tolerance value of the human body to vertical acceleration is −15–25 g. The acceleration measured at the six acceleration measuring points of the cabin guide rail selected in this study was within this range. Therefore, although the presence of cargo luggage increases the overload suffered by passengers in a vertical crash, it remains within the safe range, and the influence of seats and cushions in a vertical crash was not considered in this study; therefore, the result is still safe.

## 6. Conclusions

In this study, compression tests on cargo compartment luggage were performed, and an FEM of cargo luggage was established using HYPERMESH. The material model was crushable foam from LS-DYNA. Then, an FEM of the fuselage segment with and without cargo luggage was established. By comparing and analyzing the deformation, acceleration, displacement, and energy absorption of the fuselage section, as well as the overload response of the cabin seat rail of the fuselage section, of the two models during a vertical crash, the impact of cargo luggage on the fuselage section crash response was studied. The following conclusions are drawn.

(1) The vertical crash simulation process of the fuselage section agreed well with the test results. The FEM accurately simulated the fracture of the cargo floor beams. Moreover, plastic hinges were generated in the connection area between the cabin stanchion and the fuselage frame. When the velocity curve of the simulation and test reached 0 m/s, the times were 115 and 122 ms, respectively, with a difference of only 7 ms. The initial peak acceleration values of the simulation at C1 and C4 were 8.6% and 0.5% higher than those of the test, respectively;

(2) During the vertical crash, the cargo floor without cargo luggage was lifted to come in contact with the cabin floor and could easily penetrate the cabin floor, consequently threatening passenger safety. However, including cargo ensured that the deformation of the cargo floor with the cargo luggage was less than that of the cargo floor without cargo luggage; the deformation of the cargo floor did not affect passenger safety. Cargo luggage has a certain energy absorption and buffering effect, and the vertical displacement of the fuselage section with cargo luggage is less than that without it, thereby effectively ensuring the integrity of the living space of passengers in the cabin structure;

(3) Cargo luggage, fuselage frames, fasteners, and skin were the main energy absorption components, and the absorption of energy of cargo luggage was the largest of all components, accounting for 39.2% of the total energy absorption. The energy absorption of the fuselage frames, fasteners, and skin accounted for 13.9%, 11.4%, and 10.3%, respectively.

**Author Contributions:** Conceptualization, S.Z. and M.T.; methodology, K.L. and X.X.; validation, S.Z., Y.Z., and Y.L.; formal analysis, K.L.; investigation, X.X.; resources, X.L.; data curation, S.Z.; writing—original draft preparation, K.L.; writing—review and editing, K.L. and S.Z.; visualization, Y.Z.; supervision, Y.L.; project administration, M.T.; funding acquisition, M.T. All authors have read and agreed to the published version of the manuscript.

**Funding:** This research was supported by a research grant for MJ-2017-F15 civil aircraft crashworthiness for a basic research project.

**Institutional Review Board Statement:** Not applicable.

**Informed Consent Statement:** Not applicable.

**Data Availability Statement:** The data presented in this study are available on request from the corresponding author. The data are not publicly available due to privacy.

**Acknowledgments:** The authors gratefully acknowledge the reviewers for their careful work and thoughtful suggestions, which have helped improve this paper substantially. Special thanks to Mingbo Tong's guidance and Shuhua Zhu's revision.

**Conflicts of Interest:** The authors declare no conflict of interest.

## Abbreviations

The following abbreviations are used in this manuscript:

| | |
|---|---|
| $\sigma_{ij}$ | Stress tensor |
| $\epsilon_{ij}$ | Strain tensor |
| $n$ | Cycle number |
| $\Delta t$ | Time increment |
| $E$ | Young's modulus |
| $\sigma_i$ | Principal stress |
| $\sigma_y$ | Yield stress |
| $\rho$ | Material density |
| $E_T$ | Tangent modulus |
| $\epsilon_y$ | Failure strain for eroding elements |

## References


1. Mou, H.; Xie, J.; Feng, Z. Research status and future development of crashworthiness of civil aircraft fuselage structures: An overview. *Prog. Aerosp. Sci.* **2020**, *119*, 100644. [CrossRef]
2. Guida, M. Advances in crash dynamics for aircraft safety. *Prog. Aerosp. Sci.* **2018**, *98*, 106–123. [CrossRef]
3. Taher, S.T.; Mahdi, E.; Mokhtar, A.S.; Magid, D.L.; Ahmadun, F.R.; Prithvi, R.A. A new composite energy absorbing system for aircraft and helicopter. *Compos. Struct.* **2006**, *75*, 14–23. [CrossRef]
4. Waimer, M.; Siemann, M.H.; Feser, T. Simulation of CFRP components subjected to dynamic crash loads. *Int. J. Impact Eng.* **2016**, *101*, 115–131. [CrossRef]
5. Williams, M.S.; Hayduk, R.J. Vertical drop test of a transport fuselage section located aft of the wing. *NASA Tech. Memo.* **1983**, *85679*, 1–24.
6. Abramowitz, A.; Vu, T.; Smith, T. Vertical drop test of a narrow-body transport fuselage section with a conformable auxiliary fuel tank onboard. In *SAE Technical Paper*; SAE: Warrendale, PA, USA, 2002.
7. LePage, F.; Carciente, R. A320 fuselage section vertical drop test, part 2: Test results. *CEAT Test Rep. S* **1995**, *95*, 5776.
8. Gransden, D.I.; Alderliesten, R. Development of a finite element model for comparing metal and composite fuselage section drop testing. *Int. J. Crashworthiness* **2017**, *22*, 401–414. [CrossRef]
9. Perez Galan, J.L.; Climent, H.; Le Page, F. Non-linear response of metallic and composite aeronautical fuselage structures under crash loads and comparison with full scale test. In Proceedings of the European Congress on Computational Methods in Applied Sciences and Engineering, Barcelona, Spain, 11–14 September 2000; Volume 22, pp. 1–20.
10. Kumakura, I.; Minegishi, M.; Iwasaki, K.; Shoji, H.; Yoshimoto, N.; Terada, H.; Sashikuma, H.; Isoe, A.; Yamaoka, T.; Katayama, N.; et al. Vertical Drop Test of a Transport Fuselage Section. *J. Aerosp.* **2003**, *112*, 531–540.
11. Jackson, K.E.; Littell, J.D.; Annett, M.S.; Haskin, I.M. Finite element simulations of two vertical drop tests of F-28 fuselage sections. In *Finite Element Simulations of Two Vertical Drop Tests of F-28 Fuselage Sections*; Publishing House: Arlington, VA, USA, 2018.
12. Liu, X.C.; Zhou, S.F.; Ma, J.F. Correlation study of crash analysis and test of civil airplane sub-floor energy absorption structure. *Acta Aeronaut. Astronaut. Sin.* **2012**, *33*, 2202–2210.
13. Liu, X.C.; Guo, J.; Sun, X.S. Drop test and structure crashworthiness evaluation of civil airplane fuselage section with cabin interior. *Acta Aeronaut. Astronaut. Sin.* **2013**, *34*, 2130–2140.
14. Zheng, J.Q.; Xiang, J.W.; Luo, Z.P. Crashworthiness design of transport aircraft subfloor using polymer foams. *Int. J. Crashworthiness* **2011**, *16*, 375–383. [CrossRef]
15. Nassiraei, H.; Yara, A. Static Strength of Tubular K-Joints Reinforced with Outer Plates under Axial Loads at Ambient and Fire Conditions. *Metals* **2023**, *13*, 1857. [CrossRef]
16. Xie, J.; Mou, H.L.; Zou, T.C. Simulation analysis of cargo loading on the crashworthiness of composite fuselage section. *Mech. Strength* **2017**, *39*, 100–105.
17. Hossein, T.; Arameh, E. Quasi-static axial crush response and energy absorption of composite wrapped metallic thin-walled tube. *J. Braz. Soc. Mech. Sci. Eng.* **2022**, *44*, 158.
18. Zhu, X.F. Analysis and Evaluation of Falling Suitability of Typical Airframe Segments of Civil Aircraft. *Mech. Strength* **2017**, *39*, 100–105.


**Disclaimer/Publisher's Note:** The statements, opinions and data contained in all publications are solely those of the individual author(s) and contributor(s) and not of MDPI and/or the editor(s). MDPI and/or the editor(s) disclaim responsibility for any injury to people or property resulting from any ideas, methods, instructions or products referred to in the content.